LETTER

doi:10.1038/nature19358

A blue-light photoreceptor mediates the feedback regulation of photosynthesis

Dimitris Petroutsos[1]*, Ryutaro Tokutsu[2,3,4]*, Shinichiro Maruyama[5], Serena Flori[1], Andre Greiner[6], Leonardo Magneschi[1,7], Loic Cusant[1], Tilman Kottke[8], Maria Mittag[9], Peter Hegemann[6], Giovanni Finazzi[1] & Jun Minagawa[2,3,4]

In plants and algae, light serves both as the energy source for photosynthesis and a biological signal that triggers cellular responses via specific sensory photoreceptors. Red light is perceived by bilin-containing phytochromes and blue light by the flavin-containing cryptochromes and/or phototropins (PHOTs)[1], the latter containing two photosensory light, oxygen, or voltage (LOV) domains[2]. Photoperception spans several orders of light intensity[3], ranging from far below the threshold for photosynthesis to values beyond the capacity of photosynthetic CO_2 assimilation. Excess light may cause oxidative damage and cell death, processes prevented by enhanced thermal dissipation via high-energy quenching (qE), a key photoprotective response[4]. Here we show the existence of a molecular link between photoreception, photosynthesis, and photoprotection in the green alga *Chlamydomonas reinhardtii*. We show that PHOT controls qE by inducing the expression of the qE effector protein LHCSR3 (light-harvesting complex stress-related protein 3) in high light intensities. This control requires blue-light perception by LOV domains on PHOT, LHCSR3 induction through PHOT kinase, and light dissipation in photosystem II via LHCSR3. Mutants deficient in the *PHOT* gene display severely reduced fitness under excessive light conditions, indicating that the sensing, utilization, and dissipation of light is a concerted process that plays a vital role in microalgal acclimation to environments of variable light intensities.

In oxygenic photosynthesis, the absorption of light by pigments such as chlorophylls and carotenoids that are embedded in the light-harvesting complexes (LHCs) facilitates the transfer of energy to reaction centres, triggers electron flow from H_2O to NADPH and generates a proton motive force across the thylakoid membranes of chloroplasts that is used to drive ATP synthesis. The ATP and NADPH molecules that are generated are utilised in CO_2 fixation in the Calvin–Benson cycle[5]. Whenever light is absorbed beyond the CO_2-assimilation capacity, over-excitation of the photosystems leads to photodamage and possibly cell death. These negative consequences are prevented by non-photochemical quenching (NPQ), an intricate photoprotective process that dissipates excess absorbed energy. The major component of NPQ is qE, which occurs at the LHCs of photosystem II (ref. 6).The process of qE is driven by acidification of the thylakoid lumen that occurs under excess light, a process that modifies the pigment composition of LHCII via the xanthophyll cycle and activates specific qE protein effectors[7]. In the active state, these protein effectors (PSBS in plants and LHCSR proteins in green algae[8,9]) increase the energy dissipation capacity of LHCII via an unresolved mechanism[10,11]. Whereas plants constitutively express PSBS, the green alga *C. reinhardtii* only accumulates LHCSR3 (the major qE effector) following environmental stresses such as excess light and nutrient starvation[12]. Induction of LHCSR3 requires Ca^{2+} signalling and active photosynthesis[13,14], but the molecular mechanism behind this process is largely unknown.

To gain insight into how LHCSR3 induction is regulated, we measured the light-colour dependency (action spectrum) of qE induction in *C. reinhardtii*. Low-light-acclimated cells were exposed for 4 h to highly intense monochromatic light at different wavelengths between 400 nm and 720 nm, provided by the Okazaki Large Spectrograph[15], to induce LHCSR3. The kinetics of NPQ development were then followed under saturating white light for 5 min (Fig. 1a). The extent of NPQ observed at the end of illumination was used to evaluate the action spectrum of qE (Fig. 1b), corresponding to the fraction of NPQ that is rapidly reversible in the dark. This spectrum was comparable to the spectrum of LHCSR3 accumulation (Fig. 1c), confirming the close relationship between energy dissipation and LHCSR3 induction in this alga[8]. We found that blue light was more effective than red light in inducing the qE response (Fig. 1a, b) and LHCSR3 accumulation (Fig. 1c), although the cells absorbed both almost equally (Fig. 1b, grey area). This finding suggested that a blue-light-absorbing molecule (likely to be a blue-light receptor) is involved in the accumulation of LHCSR3 in high light intensities. To test this hypothesis we compared the kinetics of NPQ (Fig. 1a), the action spectra of qE (Fig. 1b) and the induction of LHCSR3 (Fig. 1c) in wild-type *C. reinhardtii* cells and in mutants lacking blue-light receptors—either the animal-like cryptochrome (aCRY)[16], or PHOT[17]. We found that *acry* mutant cells (deficient in a functional *ACRY* gene, hereafter *acry*) (Extended Data Fig. 1a) showed wild-type levels of qE (Fig. 1b) and LHCSR3 accumulation (Fig. 1c) throughout the entire light spectrum, including red light, where aCRY acts[16] in the absence of phytochromes in *C. reinhardtii*[18]. Conversely, *phot* mutant cells (deficient in a functional *PHOT* gene, hereafter *phot*; Extended Data Fig. 1b) specifically lacked blue-light induction of qE (Fig. 1b) and LHCSR3 accumulation (Fig. 1c), and therefore were more prone to photodamage (Fig. 1d). Induction of LHCSR3 and NPQ in response to high-intensity white light was also largely compromised in *phot* cells, in contrast to wild-type and *acry* cells (Extended Data Fig. 1c–e). The ability of *phot* cells to accumulate photoprotective carotenoids via the xanthophyll cycle was, however, similar to that of wild-type and *acry* cells (Extended Data Fig. 1f, g). The phenotype of *phot* cells was similar to that of *npq4* cells ((cells deficient in functional *LHCSR3.1* and *LHCSR3.2* genes[8]); Fig. 1b, d), that we used as a qE-lacking strain. PHOT-mediated blue-light control of LHCSR3 accumulation was

[1]Laboratoire de Physiologie Cellulaire et Végétale, UMR 5168, Centre National de la Recherche Scientifique, Commissariat à l'Energie Atomique et aux Energies Alternatives, Université Grenoble Alpes, Institut National Recherche Agronomique, Institut de Biosciences et Biotechnologies de Grenoble, (BIG), CEA Grenoble, F-38054 Grenoble CEDEX 9, France. [2]Division of Environmental Photobiology, National Institute for Basic Biology, Nishigonaka 38, Myodaiji, Okazaki 444-8585, Japan. [3]Department of Basic Biology, School of Life Science, Graduate University for Advanced Studies, Okazaki 444-8585, Japan. [4]Core Research for Evolutional Science and Technology, Japan Science and Technology Agency, Saitama 332-0012, Japan. [5]Department of Environmental Life Sciences, Graduate School of Life Sciences, Tohoku University, Sendai 980-8578, Japan. [6]Humboldt University of Berlin, Institute of Biology, Experimental Biophysics, Invalidenstraße 42, D-10115 Berlin, Germany. [7]Institute of Plant Biology and Biotechnology, University of Münster, Münster 48143, Germany. [8]Physical and Biophysical Chemistry, Bielefeld University, 33615 Bielefeld, Germany. [9]Institute of General Botany and Plant Physiology, Friedrich Schiller University, 07743 Jena, Germany.
*These authors contributed equally to this work.

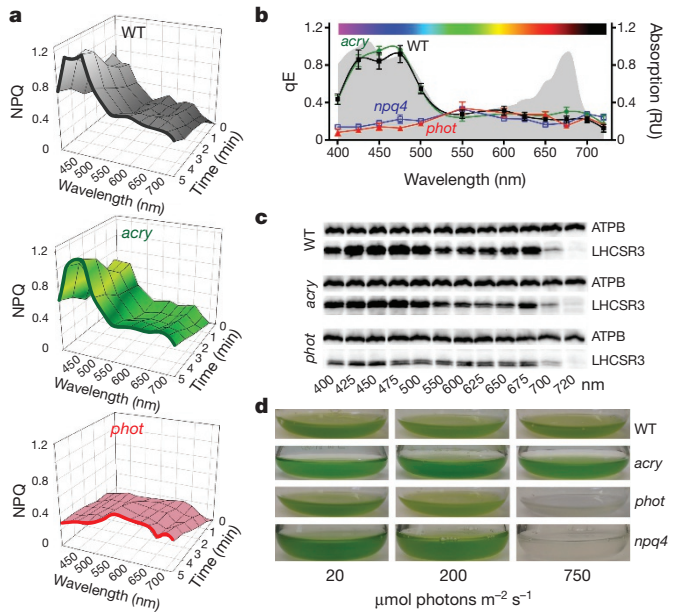

Figure 1 | PHOT controls induction of LHCSR3 and qE and is crucial for survival of *C. reinhardtii* in high light. a, NPQ in wild-type (137c), *phot* and *acry* cells after exposure for 4 h to different wavelengths of light (250 µmol photons $m^{-2} s^{-1}$). Representative dataset of an experiment replicated three times on different biological samples. **b**, qE induction in wild-type (WT; black), *acry* (green) *npq4* (blue) and *phot* (red) strains by 4 h illumination with different wavelengths of light (250 µmol photons $m^{-2} s^{-1}$). $n = 3$ biological samples, mean ± s.d. Grey area, absorption spectrum of wild-type cells. RU, relative units. **c**, Immunoblot analysis of LHCSR3 accumulation (ATPB is the loading control). Representative dataset of an experiment replicated three times on different biological samples. **d**, Erlenmeyer flasks containing wild-type, *acry*, *phot* and *npq4* cells after 16 h of exposure to light of 20, 200 and 750 µmol photons $m^{-2} s^{-1}$. Representative photographs from three biological replicates.

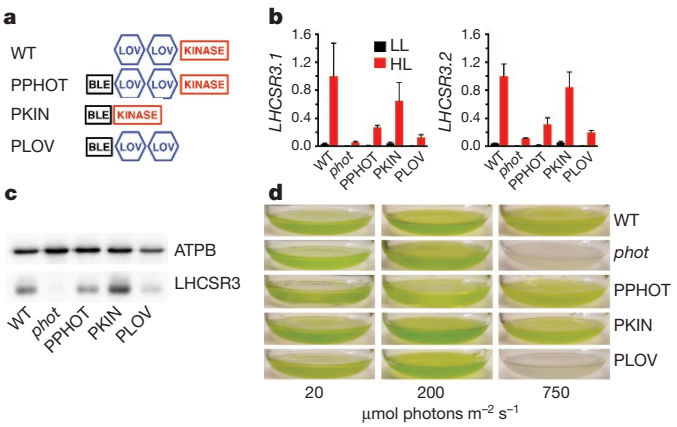

Figure 2 | Role of the different PHOT domains in controlling LHCSR3. **a**, Domains of the *PHOT* gene in wild-type and complemented *phot* lines. LOV, photosensory domain; KINASE, kinase domain; BLE, bleomycin resistance cassette. **b**, *LHCSR3.1* and *LHCSR3.2* mRNA accumulation in wild-type (cw15-302), *phot*, and variously *phot*-complemented lines exposed to low or high light intensities (LL or HL, respectively). Values relative to an endogenous control gene (*GBLP*) were normalized to wild-type samples under high light intensity ($n = 3$ biological samples, mean ± s.d.). **c**, Immunoblot analysis of LHCSR3 in wild-type and *phot* mutants (ATPB is the loading control). Representative dataset of an experiment replicated six times on different biological samples. **d**, Erlenmeyer flasks containing wild-type, *phot*, PPHOT, PKIN and PLOV strains after 20 h exposure to light of 20, 200 or 750 µmol photons $m^{-2} s^{-1}$. Representative pictures from four biological replicates.

highly specific. Accumulation of the representative subunits of the major photosynthetic complexes was comparable in all cell lines and was wavelength-insensitive (Extended Data Fig. 2a, b). The photosynthetic electron transport rate (ETR) was reduced in *phot* cells, especially upon high light exposure (Extended Data Fig. 1h, i). As photosynthesis is required for proper LHCSR3 accumulation[13,14], the lower electron flow capacity of *phot* cells could diminish LHCSR3 induction. To evaluate this hypothesis, we titrated the ETR in wild-type cells using increasing concentrations of the herbicide 3-(3,4-dichlorophenyl)-1,1-dimethylurea (DCMU), an inhibitor of electron transfer in photosystem II. The graduated addition of DCMU progressively reduced the ETR to a much lower extent in wild-type cells than in DCMU-free *phot* cells (Extended Data Fig. 3a). However, accumulation of LHCSR3 remained greater in DCMU-treated wild-type cells than in DCMU-untreated *phot* cells (Extended Data Fig. 3b). We therefore excluded the possibility that the diminished ETR observed in *phot* cells was the cause of the impaired LHCSR3 accumulation. We concluded instead that the impaired photoprotection in *phot* cells was the cause of the reduced ETR (Extended Data Fig. 1i) and enhanced photosensitivity (Fig. 1d), indicating that PHOT is a central actor of photoprotection in this alga.

Phototropins are ubiquitous in plants and algae. Their function in light perception involves two structurally similar LOV domains (LOV1 and LOV2) at the N terminus and downstream signalling via a C-terminal serine/threonine kinase domain[2]. We dissected the role of the different PHOT domains in LHCSR3-induction using existing mutants[19] (Fig. 2a). Complementation of *phot* cells with the full-length *phot* cDNA (giving the PPHOT strain) restored PHOT protein expression (Extended Data Fig. 4a), expression of *LHCSR3.1* and *LHCSR3.2* transcripts (both of which encode LHCSR3 (ref. 8; Fig. 2b) and expression of LHCSR3 protein (Fig. 2c) to a limited extent. This partial restoration was nonetheless sufficient to largely rescue resistance to high-light-induced stress (Fig. 2d and Extended Data Fig. 4b). Moreover, introduction of the *LHCSR3.1* gene into *phot* cells under the control of the strong, *PHOT*-independent *PSAD* promoter (the PLHCSR3 strain) also rescued qE and LHCSR3 levels (Extended Data Fig. 5). This therefore confirmed the univocal relationship between PHOT, LHCSR3 and photoprotection. Conversely, complementation of *phot* cells with truncated gene carrying only the photosensory domains LOV1 and LOV2 (giving the PLOV strain) did not rescue either protein expression or photosensitivity (Fig. 2c, d and Extended Data Fig. 4b). Finally, complementation with the kinase domain of PHOT (giving the PKIN strain) fully restored expression of LHCSR3 and photoprotection (Fig. 2c, d and Extended Data Fig. 4b). In this strain, however, LHCSR3 accumulation became light–colour-independent (Fig. 3a, b), in contrast to the wild-type (Fig. 1a, c) and the PPHOT (Fig. 3a, b) strain. This indicates that removal of the LOV domains leads to the loss of inhibition of the kinase activity, as has been previously reported in plants[20]. Deregulation of the PHOT kinase activity (as in the PKIN strain) or removal of the kinase domain (as in *phot* cells and in PLOV) did not alter LHCSR3 phosphorylation levels (Extended Data Fig. 6), ruling out any link between PHOT and LHCSR3 phosphorylation. We also found that LHCSR3 accumulation remained light-intensity-dependent in the PKIN strain (Fig. 3c, d), suggesting that in addition to PHOT, high-light-intensity photosynthesis was required for the accumulation of LHCSR3. In another mutant, generated by inserting an additional copy of the kinase domain into wild-type *C. reinhardtii* cells (giving the WTKIN strain; Extended Data Fig. 7a–d), LHCSR3 accumulation also became largely wavelength-independent but was still sensitive to light intensity. Moreover, accumulation of LHCSR3 was completely blocked upon inhibition of photosynthesis by DCMU in the PKIN and WTKIN strains (Fig. 3c, d and Extended Data Fig. 7e). Additionally, LHCSR3 was not accumulated under light from the far-red part of the spectrum (720 nm) in each cell line (Figs 1c, 3a, b and Extended Data Fig. 7c, d). This light is not absorbed by *C. reinhardtii* cells (Fig. 1b, grey area) and therefore does not activate photosynthesis.

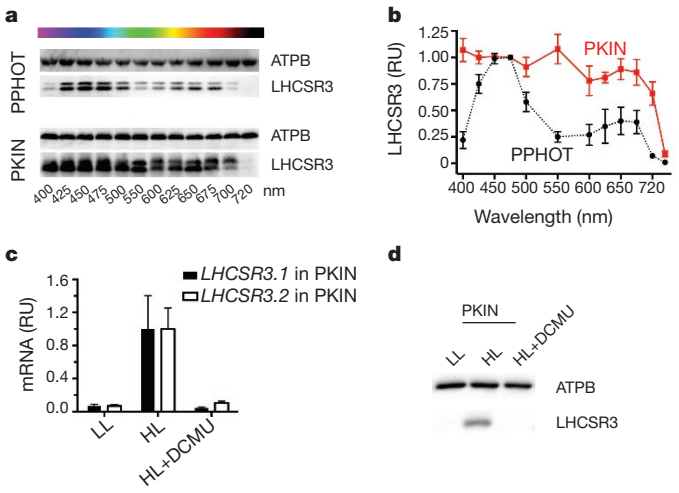

Figure 3 | PHOT-dependent control of LHCSR3 expression requires blue light perception by LOV, signal transduction by the C-terminal kinase domain of PHOT and photosynthesis. a, Action spectrum of LHCSR3 accumulation in PPHOT and PKIN (ATPB is the loading control). Representative dataset of an experiment replicated three times on different biological samples. **b**, Densitometric quantification of LHCSR3 accumulation of Fig. 3a. Values are normalized to 475 nm ($n = 3$ biological samples, mean ± s.d.). **c**, *LHCSR3.1* and *LHCSR3.2* mRNA accumulation in PKIN at low light intensity and at high light intensity in the presence and absence of the PSII inhibitor DCMU. Values are normalized to high light intensity ($n = 3$ biological samples, mean ± s.d.). **d**, LHCSR3 protein accumulation in PKIN at low and high light intensity in the presence or absence of DCMU for 4 h. Representative dataset of an experiment replicated three times on different biological samples.

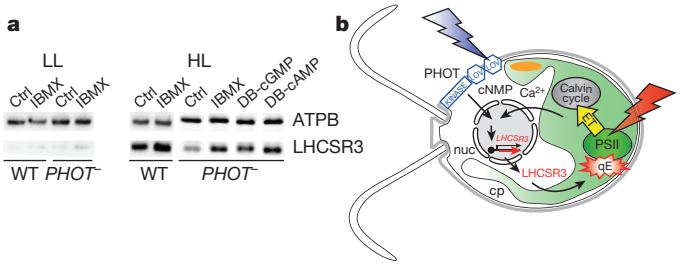

Figure 4 | Possible signal transduction pathway for high-light-intensity-induced expression of LHCSR3. a, Immunoblot analyses of LHCSR3 accumulation in wild-type (cw15-302) and *phot* cells treated with the phosphodiesterase inhibitor IBMX, DB-cAMP or DB-cGMP after 20 h at low or high light intensities. Representative dataset of an experiment replicated five times on different biological samples. Ctrl, control. **b**, Schematic representation of the relationship between photoreception, photosynthesis and -photoprotection in *C. reinhardtii*. cp, chloroplast; cNMP, cyclic nucleotide mono phosphate (cAMP or cGMP); ET, electron transport; eye, eyespot; nuc, nucleus; PSII, photosystem II.

In *Arabidopsis thaliana*, PHOT proteins regulate the blue-light-induced increase in cytosolic free Ca^{2+} (refs 21, 22). As PHOT controls LHCSR3 expression in *C. reinhardtii* (Fig. 1) and Ca^{2+} is required for the accumulation of LHCSR3 (ref. 13), a relationship between PHOT, Ca^{2+}, and LHCSR3 can be conceived. However, a tenfold increase in extracellular Ca^{2+} (to 3.4 mM) did not restore LHCSR3 accumulation in the *phot* mutant (Extended Data Fig. 8a). This finding led us to conclude that Ca^{2+} signalling is not modulating LHCSR3 in the absence of PHOT. We propose that other second messengers, such as the cyclic nucleotides cAMP or cGMP, act as the signalling molecules downstream of PHOT. We tested this using a pharmacological approach and found that treatment of *phot* cells with 3-isobutyl-1-methylxanthine (IBMX), an inhibitor of cAMP and cGMP phosphodiesterases, rescued LHCSR3 expression (Fig. 4a and Extended Data Fig. 8b). We confirmed this effect by incubating *phot* cells with dibutyrylated cGMP and cAMP (DB-cGMP and DB-cAMP; Fig. 4a), suggesting that cyclic nucleotides are not only critical in mating and phototaxis[18], but are also involved in photoprotection in *C. reinhardtii* through the regulation of LHCSR3 expression. On the other hand, induction of LHCSR3 in IBMX-treated wild-type or *phot* cells remained light-intensity-dependent (Fig. 4a), indicating that cAMP and/or cGMP require a high-light-photosynthesis-related signal to be effective on LHCSR3 accumulation.

Extensive research has focused on the nature and function of the molecular actors involved in the sensing (by photoreceptors) and utilization (by photosynthetic complexes) of environmental light. Our findings here uncover the molecular linkage between these two essential functions of photosynthetic organisms (Fig. 4b). Blue light perceived by PHOT mediates the photoprotection of the photosynthetic machinery (qE) in a green alga. The LOV domains of PHOT provide blue-light sensitivity while the C-terminal kinase domain performs signal transduction, possibly via the initiation of a cyclic nucleotide monophosphate signalling cascade. Downstream of PHOT, this signal integrates with another regulatory signal from the chloroplast that carries information about the amount of absorbed light that is not used for CO_2 fixation. This signal relies on photosynthetic electron transfer[13,14] via an as-yet-unknown mechanism. The integrated signal affects accumulation of *LHCSR3.1* and *LHCSR3.2* transcripts (Fig. 2b), primarily owing to the activation of transcription and partially to the stabilization of the transcripts (Extended Data Fig. 9). This contrasts with plant PHOT proteins that have been suggested to destabilize transcripts[23], while little evidence exists for their role in activation of transcription[2]. The LHCSR3 polypeptide is then imported into the chloroplast thylakoids, where it modulates qE (Fig. 4b).

Because LHCSR3 is an ancient light-harvesting protein[8] found only in lower plants including green unicellular eukaryotic algae (chlorophytes) and mosses[7], as well as in some algae with secondary plastids, we propose that the molecular link between photoreception, photosynthesis, and photoprotection discovered in this study has evolved in the environment in which photosynthesis originated during evolution—namely the water columns—where blue light dominates the available spectrum. Consistent with this hypothesis, photoprotection in cyanobacteria, which are thought to share a common ancestry with chloroplasts, also relies on blue light. The cyanobacterial NPQ protein effector OCP (orange carotenoid protein) binds a single blue-light-absorbing carotenoid. NPQ in cyanobacteria is also triggered by high-intensity blue light[24]. Evidences also show a link between blue light and photoprotection in diatoms[25] via an uncharacterized mechanism. On the other hand, the blue-light-dependent control of photoprotection was apparently lost during land-colonization. Here, a new qE process evolved reliant on the constitutively expressed protein PsbS[4]. Land plants, however, seem to carry a remnant of ancestral qE control by blue light, named qM, as blue light still affects NPQ in these organisms, but only via the PHOT-triggered chloroplast avoidance movement that helps chloroplasts to avoid high light intensities[26].

The transition from water to land was paralleled by the emergence of a second *PHOT* gene. Seed plants express both PHOT1, a protein that responds to low-intensity blue light signals, and PHOT2, a protein that triggers high-intensity blue light responses. Unicellular green algae such as *Chlorella variabilis*, *Ostreococcus tauri* and *C. reinhardtii* only contain one *PHOT* gene, an orthologue of *PHOT2* (ref. 27). However, in *C. reinhardtii* blue light triggers different biological responses depending on the photon fluence rate. Low-intensity blue light (for example, 1 μmol photons $m^{-2} s^{-1}$) triggers gametogenesis at low nitrogen abundance[28] and gene expression[29] whereas blue light at higher intensities desensitizes the eyespot[19] and induces LHCSR3 expression (for example, 60 μmol photon $m^{-2} s^{-1}$, Extended Data Fig. 10a, b). Thus, we conclude that the same PHOT protein that ensures responses at low light intensities can trigger signalling at higher light intensities when acting in synergy with the photosynthetic signal. We propose that, although the transition from motility (algae) to

sessility (land plants) led to an increase in specialization of the function of photoreceptors, this process occurred at the expense of some essential functions in water, probably the regulation of photoprotection that is reported here.

Online Content Methods, along with any additional Extended Data display items and Source Data, are available in the online version of the paper; references unique to these sections appear only in the online paper.

Received 3 December 2015; accepted 11 August 2016.
Published online 14 August 2016.

1. Jiao, Y., Lau, O. S. & Deng, X. W. Light-regulated transcriptional networks in higher plants. *Nat. Rev. Genet.* **8,** 217–230 (2007).
2. Christie, J. M. Phototropin blue-light receptors. *Annu. Rev. Plant Biol.* **58,** 21–45 (2007).
3. Briggs, W. R. Phototropism: some history, some puzzles, and a look ahead. *Plant Physiol.* **164,** 13–23 (2014).
4. Li, Z., Wakao, S., Fischer, B. B. & Niyogi, K. K. Sensing and responding to excess light. *Annu. Rev. Plant Biol.* **60,** 239–260 (2009).
5. Eberhard, S., Finazzi, G. & Wollman, F. A. The dynamics of photosynthesis. *Annu. Rev. Genet.* **42,** 463–515 (2008).
6. Horton, P., Ruban, A. V. & Walters, R. G. Regulation of light harvesting in green plants. *Annu. Rev. Plant Physiol. Plant Mol. Biol.* **47,** 655–684 (1996).
7. Niyogi, K. K. & Truong, T. B. Evolution of flexible non-photochemical quenching mechanisms that regulate light harvesting in oxygenic photosynthesis. *Curr. Opin. Plant Biol.* **16,** 307–314 (2013).
8. Peers, G. *et al.* An ancient light-harvesting protein is critical for the regulation of algal photosynthesis. *Nature* **462,** 518–521 (2009).
9. Tokutsu, R. & Minagawa, J. Energy-dissipative supercomplex of photosystem II associated with LHCSR3 in *Chlamydomonas reinhardtii*. *Proc. Natl Acad. Sci. USA* **110,** 10016–10021 (2013).
10. Ruban, A. V. *et al.* Identification of a mechanism of photoprotective energy dissipation in higher plants. *Nature* **450,** 575–578 (2007).
11. Ahn, T. K. *et al.* Architecture of a charge-transfer state regulating light harvesting in a plant antenna protein. *Science* **320,** 794–797 (2008).
12. Finazzi, G. & Minagawa, J. in *Non-PHOTochemical Quenching and Energy Dissipation in Plants, Algae and Cyanobacteria* (eds Demmig-Adams, B., Garab, G., Adams, W. III & Govindjee) Ch 21, 445–469 (Springer Netherlands, 2014).
13. Petroutsos, D. *et al.* The chloroplast calcium sensor CAS is required for photoacclimation in *Chlamydomonas reinhardtii*. *Plant Cell* **23,** 2950–2963 (2011).
14. Maruyama, S., Tokutsu, R. & Minagawa, J. Transcriptional regulation of the stress-responsive light harvesting complex genes in *Chlamydomonas reinhardtii*. *Plant Cell Physiol.* **55,** 1304–1310 (2014).
15. Watanabe, M. *et al.* Design and performance of the Okazaki large spectrograph for photobiological research. *Photochem. photobiol.* **36,** 491–498 (1982).
16. Beel, B. *et al.* A flavin binding cryptochrome photoreceptor responds to both blue and red light in *Chlamydomonas reinhardtii*. *Plant Cell* **24,** 2992–3008 (2012).
17. Zorin, B., Lu, Y., Sizova, I. & Hegemann, P. Nuclear gene targeting in *Chlamydomonas* as exemplified by disruption of the *PHOT* gene. *Gene* **432,** 91–96 (2009).
18. Merchant, S. S. *et al.* The *Chlamydomonas* genome reveals the evolution of key animal and plant functions. *Science* **318,** 245–250 (2007).
19. Trippens, J. *et al.* Phototropin influence on eyespot development and regulation of phototactic behavior in *Chlamydomonas reinhardtii*. *Plant Cell* **24,** 4687–4702 (2012).
20. Kong, S.-G. *et al.* The C-terminal kinase fragment of *Arabidopsis* phototropin 2 triggers constitutive phototropin responses. *Plant J.* **51,** 862–873 (2007).
21. Harada, A., Sakai, T. & Okada, K. phot1 and phot2 mediate blue light-induced transient increases in cytosolic Ca^{2+} differently in *Arabidopsis* leaves. *Proc. Natl Acad. Sci. USA* **100,** 8583–8588 (2003).
22. Babourina, O., Newman, I. & Shabala, S. Blue light-induced kinetics of H^+ and Ca^{2+} fluxes in etiolated wild-type and phototropin-mutant *Arabidopsis* seedlings. *Proc. Natl Acad. Sci. USA* **99,** 2433–2438 (2002).
23. Folta, K. M. & Kaufman, L. S. Phototropin 1 is required for high-fluence blue-light-mediated mRNA destabilization. *Plant Mol. Biol.* **51,** 609–618 (2003).
24. Kirilovsky, D. & Kerfeld, C. A. The orange carotenoid protein: a blue-green light photoactive protein. *Photochem. photobiol. Sci.* **12,** 1135–1143 (2013).
25. Schellenberger Costa, B. *et al.* Blue light is essential for high light acclimation and photoprotection in the diatom *Phaeodactylum tricornutum*. *J. Exp. Bot.* **64,** 483–493 (2013).
26. Cazzaniga, S., Dall' Osto, L., Kong, S. G., Wada, M. & Bassi, R. Interaction between avoidance of photon absorption, excess energy dissipation and zeaxanthin synthesis against photooxidative stress in *Arabidopsis*. *Plant J.* **76,** 568–579 (2013).
27. Galván-Ampudia, C. S. & Offringa, R. Plant evolution: AGC kinases tell the auxin tale. *Trends Plant Sci.* **12,** 541–547 (2007).
28. Huang, K. & Beck, C. F. Phototropin is the blue-light receptor that controls multiple steps in the sexual life cycle of the green alga *Chlamydomonas reinhardtii*. *Proc. Natl Acad. Sci. USA* **100,** 6269–6274 (2003).
29. Im, C. S., Eberhard, S., Huang, K., Beck, C. F. & Grossman, A. R. Phototropin involvement in the expression of genes encoding chlorophyll and carotenoid biosynthesis enzymes and LHC apoproteins in *Chlamydomonas reinhardtii*. *Plant J.* **48,** 1–16 (2006).

Acknowledgements We thank K. Kamada for help with genetic crossing, Y. Yari Kamrani for help with the Okazaki Large Spectrograph experiments and K. Kosuge for help with immunoblotting experiments. We thank G. Kreimer and Y. Aihara for discussions, M. Hippler for the antibody against LHCSR3 and G. Allorent for help during the initial phase of this project. We also thank P. Longoni and M. Goldschmidt-Clermont for advice and technical assistance with Phos-tag PAGE and T. Yamasaki for assistance with quantitative PCR. This work was supported by grants from Agence Nationale de la Recherche (ANR-12-BIME-0005, GRAL Labex, ANR-10-LABX-49-01, DiaDomOil to D.P. and G.F.); the Marie Curie Initial Training Network Accliphot (FP7-PEOPLE-2012-ITN; 316427 to G.F., D.P., S.F.); the CNRS Défi (ENRS 2013 to G.F. and D.P.); the CEA Bioénergies program (to G.F. and D.P.); the HFSP (HFSP0052) to G.F. and D.P.; the NIBB Cooperative Research Program for the Okazaki Large Spectrograph (13-514 and 14-508 to G.F. and 15-609 and 16-705 to J.M.); JSPS KAKENHI (JP15H05599 to R.T., JP26251033 and JP16H06553 to J.M. and R.T.); the NEDO (P07015 to J.M.); the MEXT (through the Network of Centres of Carbon Dioxide Resource Studies in Plants to J.M.); the German Research Foundation, DFG, grants FOR1261 (to P.H., M.M. and T.K.) and Heisenberg fellowship (to T.K.). L.M. acknowledges support from the Alexander von Humboldt Stiftung/ Foundation.

Author Contributions D.P., R.T., J.M. and G.F. designed the study. D.P., R.T., S.F. and L.M performed biochemical analyses; D.P. and R.T. performed fluorescence measurements; D.P. performed pharmacological tests; D.P., R.T., J.M. and G.F. performed action spectra; R.T. performed mutant generation; R.T. and S.M. performed quantitative PCR analysis; S.F. performed pigment quantification; L.C. performed the photosensitivity tests; J.M. and G.F. performed non-photochemical quenching experiments. D.P., R.T., S.M., A.G., L.M., T.K., M.M., P.H., J.M. and G.F. provided strains and analysed the data. D.P., R.T., J.M. and G.F. wrote the manuscript, and all authors revised and approved it.

Author Information Reprints and permissions information is available at www.nature.com/reprints. The authors declare no competing financial interests. Readers are welcome to comment on the online version of the paper. Correspondence and requests for materials should be addressed to D.P. (dimitris.petroutsos@cea.fr), G.F. (giovanni.finazzi@cea.fr) or J.M. (minagawa@nibb.ac.jp).

Reviewer Information *Nature* thanks J.-D. Rochaix and the other anonymous reviewer(s) for their contribution to the peer review of this work.

METHODS

No statistical methods were used to predetermine sample size. The experiments were not randomized. The investigators were not blinded to allocation during experiments and outcome assessment.

Chemicals. Chemicals were purchased from Sigma (DCMU) and Enzo (3-isobutyl-1-methylxanthine (IBMX), dibutyryl cyclic AMP (DB-cAMP), and dibutyryl cyclic GMP (DB-cGMP)). Stock solutions of DCMU were prepared in ethanol (40 mM) or H_2O (40 μM); IBMX was dissolved in DMSO at 250 mM; DB-cAMP and DB-GMP were dissolved in H_2O.

Strains and conditions. *Chlamydomonas reinhardtii* strains were grown under 20 μmol photons $m^{-2} s^{-1}$ in Tris-acetate-phosphate (TAP) media[30] at 23 °C. In all experiments cells were transferred to Sueoka's high salt medium[31] at 2 million cells ml^{-1} and exposed to light intensities as described in the text and figure legends. Two *C. reinhardtii* wild-type strains, cw15-302 and 137c, were used as indicated in the figure legends. The *phot* mutant was previously generated using a homologous recombination strategy[17]. For the different complemented lines of *phot*, *PsaD* promoter and terminator were used for the expression of full-length *PHOT* cDNA (strain PPHOT; clone PPHOT3 or PPHOT4), the LOV domains (strain PLOV; clone PLOV1) and the kinase domain (strain PKIN; clone PKIN1), N-terminally fused to the zeocin resistance marker sh-*Ble*[19]. Using the same strategy, overexpression of the PHOT kinase domain in the wild-type background resulted in the strain WTKIN[19]. For the PHOT-independent expression of LHCSR3, the *PsaD* promoter and terminator were fused to a full-length genomic *LHCSR3.1* gene. The generated construct with the *APH7* marker gene was introduced into *phot* by electroporation with NEPA21 Super Electroporator (Nepa Gene). The transformants, PLHCSR3(B5) and PLHCSR3(G6), were screened for their resistance to 10 μg ml^{-1} hygromycin. The *acry* mutant, originally delivered in a SAG73.72 genetic background[16], was backcrossed three times to wild-type strain 137c. Unless otherwise stated, low-light-intensity conditions corresponded to 20 μmol photons $m^{-2} s^{-1}$ while high-light-intensity conditions corresponded to 250 μmol photons $m^{-2} s^{-1}$ of white light. All experiments were repeated three times on different biological samples to verify their reproducibility, unless otherwise stated.

Pigment and mRNA quantification. Extraction and quantification of chlorophyll and xanthophylls, calculation of the de-epoxidation state DES, and mRNA quantification by quantitative PCR were performed as described previously[14,32]. A gene encoding G-protein-subunit-like protein (GBLP)[33] was used as the endogenous control, and relative expression values relative to *GBLP* (Figs 2b and 3c) were calculated from three biological replicates, each of which contained three technical replicates. The primers used were *LHCSR3.1* (5′-CACAACACCTTGATGCGAGATG-3′ and 5′-CCGTGTCTTGTCAGTCCCTG-3′), *LHCSR3.2* (5′-TGTGAGGCACTCTGGTGAAG-3′ and 5′-CGCCTGTTGTCACCATCTTA-3′), *GBLP* (5′-CAAGTACACCATTGGCGAGC-3′ and 5′-CTTGCAGTTGGTCAGGTTCC-3′), and 18S rRNA (5′-AGCATGAGAGATGGCTACCACATC-3′ and 5′-CATTCCAATTACCAGACGCGAAGC-3′). The mRNA stability experiments were performed in the presence of the transcription inhibitor actinomycin D (Wako) at 160 μg ml^{-1} (ref. 34). Reverse-transcription PCR was performed using Light cycler 96 (Roche) with AptaTaqDNA GM with ROX (Roche).

Immunoblotting. Protein samples of whole cell extracts (0.5 μg chlorophyll, unless stated otherwise) were loaded on 7% or 13% SDS–PAGE gels and blotted onto nitrocellulose membranes. Antisera against D1, D2 and ATPB were obtained from Agrisera; antisera against *C. reinhardtii* aCRY[16], PHOT (LOV1 domain)[17], and all others[35,36] were previously described. ATPB was used as a loading control. An anti-rabbit horseradish-peroxidase-conjugated antiserum was used for detection. The blots were developed with ECL detection reagent and images of the blots were obtained using a CCD imager (ChemiDoc MP System, Bio-Rad). For the densitometric quantification of LHCSR3, data were normalized to ATPB. LHCSR3 appears as a double band in some of the western blots (that is, Fig. 3 and Extended Data Figs 2, 4, 6–8). The upper band represents the phosphorylated form of LHCSR3 (see Extended Data Fig. 6). The extent of LHCSR3 phosphorylation was determined using a Phos-tag-based method as described[37]. For the dephosphorylation of LHCSR3, whole-cell extracts (1 μg total chlorophyll) were treated with either 20 U of calf intestine phosphatase (Promega) or 200 U of λ protein phosphatase (λPP) (New England Biolabs) in the presence of 0.05 (v/v) Triton X-100, at 30 °C for 1 h.

Fluorescence-based measurements. Fluorescence-based photosynthetic parameters were measured with a fluorescence imaging setup previously described[38]. The photosynthetic electron transfer rate was calculated as $ETR = (F_m' - F)/F_m' \times 0.84 \times 0.5 \times I$ (ref.39). qE was estimated as the fraction of NPQ that is rapidly inducible in the light and reversible in the dark, using the following equation: $qE = (F_m - F_m')/F_m'$. where F and F_m' are the fluorescence yields in steady state light and after a saturating pulse in the actinic light, respectively; F_m is the maximal fluorescence yield in dark-adapted cells; and I is the light irradiance in μmol photons $m^{-2} s^{-1}$ (ref. 40). Before NPQ measurements, cells were exposed to high-intensity light for 4 h unless stated to induce LHCSR3 and dark acclimated for 30 min. For NPQ measurements, actinic light was set at 750 μmol photons $m^{-2} s^{-1}$. For action spectra measurements, 5 ml of concentrated cells (2×10^7 cells ml^{-1}) were placed in a Petri dish and exposed to intense (250 μmol photons $m^{-2} s^{-1}$) monochromatic light (the spectral half width is 5.5 nm or less), provided by the Okazaki Large Spectrograph[15] for 4 h. Samples were then collected and subjected to immunoblotting (0.1 ml) as well as qE measurement (0.2 ml) with a fluorescence video-imaging system (Fluorocam, Photon System Instruments).

30. Gorman, D. S. & Levine, R. P. Cytochrome f and plastocyanin: their sequence in the photosynthetic electron transport chain of *Chlamydomonas reinhardi*. *Proc. Natl Acad. Sci. USA* **54,** 1665–1669 (1965).
31. Sueoka, N. Mitotic replication of deoxyribonucleic acid in *Chlamydomonas reinhardii*. *Proc. Natl Acad. Sci. USA* **46,** 83–91 (1960).
32. Allorent, G. *et al.* A dual strategy to cope with high light in *Chlamydomonas reinhardtii*. *Plant Cell* **25,** 545–557 (2013).
33. Schloss, J. A. A Chlamydomonas gene encodes a G protein β subunit-like polypeptide. *Mol. Gen. Genet.* **221,** 443–452 (1990).
34. Gera, J. F. & Baker, E. J. Deadenylation-dependent and -independent decay pathways for α1-tubulin mRNA in *Chlamydomonas reinhardtii*. *Mol. Cell. Biol.* **18,** 1498–1505 (1998).
35. Takahashi, H., Iwai, M., Takahashi, Y. & Minagawa, J. Identification of the mobile light-harvesting complex II polypeptides for state transitions in *Chlamydomonas reinhardtii*. *Proc. Natl Acad. Sci. USA* **103,** 477–482 (2006).
36. Iwai, M. *et al.* Isolation of the elusive supercomplex that drives cyclic electron flow in photosynthesis. *Nature* **464,** 1210–1213 (2010).
37. Longoni, P., Douchi, D., Cariti, F., Fucile, G. & Goldschmidt-Clermont, M. Phosphorylation of the light-harvesting complex II isoform Lhcb2 is central to state transitions. *Plant Physiol.* **169,** 2874–2883 (2015).
38. Johnson, X. *et al.* A new setup for in vivo fluorescence imaging of photosynthetic activity. *photosynth. Res.* **102,** 85–93 (2009).
39. Petroutsos, D. *et al.* PGRL1 participates in iron-induced remodeling of the photosynthetic apparatus and in energy metabolism in *Chlamydomonas reinhardtii*. *J. Biol. Chem.* **284,** 32770–32781 (2009).
40. Genty, B., Briantais, J.-M. & Baker, N. R. The relationship between the quantum yield of photosynthetic electron transport and quenching of chlorophyll fluorescence. *Biochim. Biophys. Acta* **990,** 87–92 (1989).
41. Depège, N., Bellafiore, S. & Rochaix, J. D. Role of chloroplast protein kinase Stt7 in LHCII phosphorylation and state transition in *Chlamydomonas*. *Science* **299,** 1572–1575 (2003).
42. Bergner, S. V. *et al.* STATE TRANSITION7-dependent phosphorylation is modulated by changing environmental conditions, and its absence triggers remodeling of photosynthetic protein complexes. *Plant Physiol.* **168,** 615–634 (2015).

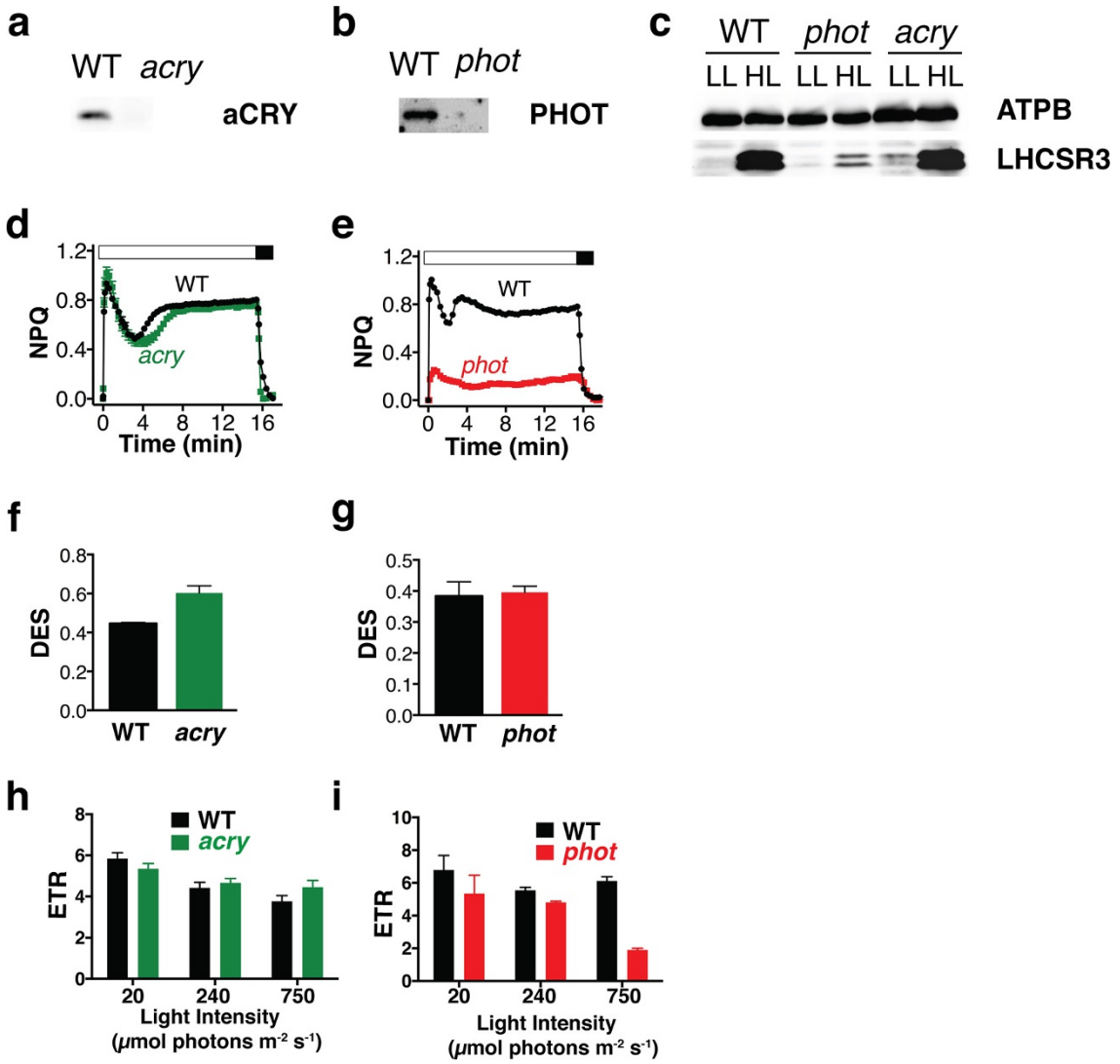

Extended Data Figure 1 | Photosynthetic properties of *acry* and *phot* mutants. a, Immunoblot analysis of aCRY accumulation in wild-type (137c) and *acry* cells. The two strains were grown as previously described[16]. Cells were harvested at the beginning of the light phase (LD2 phase[16]). Whole-cell samples with 2 μg of chlorophyll were loaded on each lane. Representative dataset of an experiment replicated 3 times on different biological samples. **b**, Immunoblot analysis of PHOT in wild-type (cw15-302) and *phot* cells after 4 h exposure to high-intensity white light. Representative dataset of an experiment replicated 3 times on different biological samples. **c**, Immunoblot analysis of LHCSR3 and ATPB in wild-type (137c), *phot* and *acry* cells in low light intensity and after 4 h exposure to high-intensity white light (HL). ATPB was used as a loading control. Representative dataset of an experiment replicated five times on different biological samples. **d**, **e**, NPQ induction kinetics of wild-type (137c) and *acry* cells (**d**) and wild-type (cw15-302) and *phot* cells (**e**) after 4 h exposure to high-intensity white light. qE was recorded for 16 min upon illumination with 440 μmol photons $m^{-2} s^{-1}$ (white bar) followed by 2 min of darkness (black bar), to measure qE relaxation. Representative dataset of an experiment replicated 4 (**d**) and 7 (**e**) times on different biological samples. **f**, **g**, DES indicates the xanthophyll cycle de-epoxidation state ([zeaxanthin] + 1/2[antheraxanthin])/([zeaxanthin] + [antheraxanthin] + [violaxanthin]) in wild-type (137c) and *acry* cells (**f**) and wild-type (cw15-302) and *phot* cells (**g**) after exposure to high light intensity for 4 h ($n = 3$ biological samples, mean ± s.d.). **h**, **i**, ETR of wild-type (137c) and *acry* (**h**) and wild-type (cw15-302) and *phot* (**i**) cells exposed at 20, 240 and 750 μmol photons $m^{-2} s^{-1}$ for 10 h. ETR (μmol photons $m^{-2} s^{-1}$) was measured at actinic illumination of 41 μmol photons $m^{-2} s^{-1}$ ($n = 3$ biological samples, mean ± s.d.).

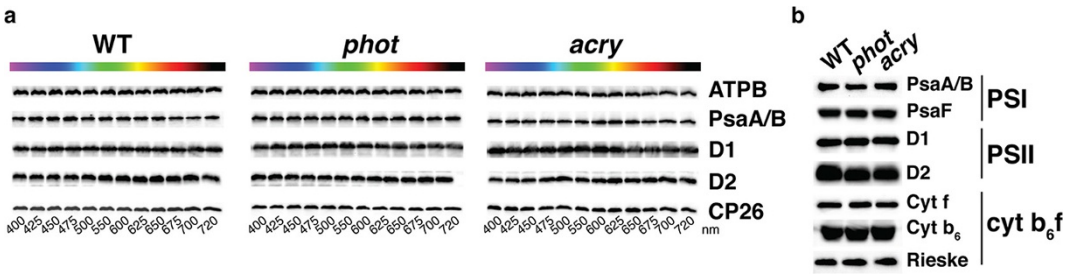

Extended Data Figure 2 | Accumulation of major photosynthetic complexes is unaltered in the *phot* cells upon exposure to different wavelengths of visible light. a, Immunoblot analyses of ATPB, PsaA/B, D1, D2 and CP26 accumulation in wild-type (137c), *phot* and *acry* cells after 4 h exposure to 250 μmol photons m^{-2} s^{-1} of monochromatic light at the different wavelengths of the visible spectrum. **b**, Immunoblot analyses of major photosynthetic complexes of PSII, cyt b_6f and PSII in wild-type, *phot* and *acry* cells after 4 h exposure at 250 μmol photons m^{-2} s^{-1} of white light. Representative dataset of an experiment replicated three times on different biological samples.

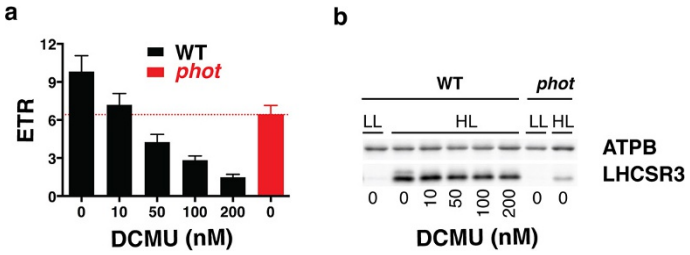

Extended Data Figure 3 | Diminished LHCSR3 induction in *phot* is not caused by diminished photosynthesis. a, Comparison of ETR in DCMU-titrated wild-type cells and DCMU-untreated *phot* cells exposed to high light intensity for 3 h. ETR (μmol photons $m^{-2} s^{-1}$) was measured upon exposure to light of 170 μmol photons $m^{-2} s^{-1}$ ($n = 3$ biological samples, mean ± s.d.). **b**, Immunoblot analyses of LHCSR3 accumulations in the wild-type and *phot* samples described in **a**. ATPB was used as a loading control. Representative dataset of an experiment replicated five times on different biological samples.

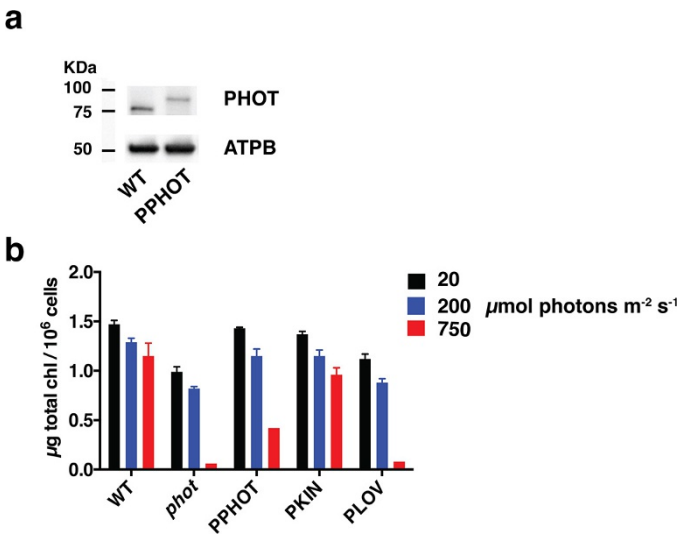

Extended Data Figure 4 | PHOT protein levels pigment content in *phot* mutants. a, Immunoblot analyses of PHOT accumulation in wild-type (cw15-302) and PPHOT strains. PPHOT expresses a fused PHOT–BLE protein, which has a higher molecular mass than wild-type PHOT. ATPB served as a loading control. Representative dataset of experiment replicated four times on different biological samples. **b**, Total cellular chlorophyll ($a+b$) content in wild-type, *phot*, PPHOT, PKIN and PLOV cells exposed to light of 20, 200 or 750 µmol photons $m^{-2}\,s^{-1}$ for 20 h as in Fig. 2d ($n=3$ biological samples, mean ± s.d.). Diminished chlorophyll content is a signature of pigment bleaching following photo-damage.

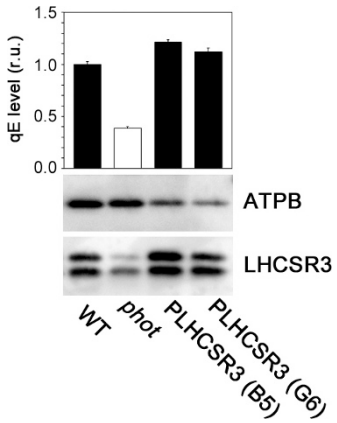

Extended Data Figure 5 | PHOT-independent LHCSR3 expression restores photoprotection in the *phot* mutant. Relative qE and LHCSR3 expression under high-light-intensity conditions in wild-type (cw15-302), *phot*, and two *phot*-transformed lines expressing an additional copy of the *LHCSR3.1* gene under the control of the *PsaD* promoter (PLHCSR3(B5) and PLHCSR3(G6)). ATPB was used as a loading control. qE values were normalized to wild-type cells ($n = 3$ biological samples, mean ± s.d.).

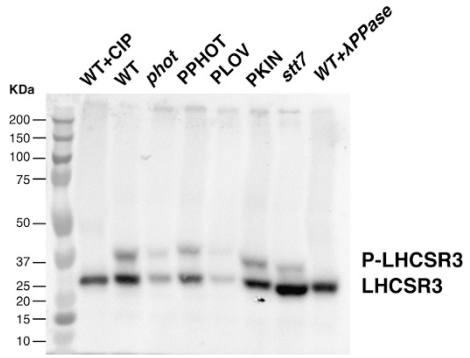

Extended Data Figure 6 | Phosphorylation levels of LHCSR3 in *phot*, PPHOT, PLOV, PKIN, *stt7* and wild-type cells. Assessment of the phosphorylation levels of LHCSR3 in wild-type (cw15-302), *phot*, PPHOT, PLOV and PKIN cells by a mobility-shift detection of phosphorylated proteins (Phos-tag). The upper and lower bands correspond to the phosphorylated and non-phosphorylated forms of LHCSR3 (P-LHCSR3 and LHCSR3), respectively, as confirmed by treatment of the samples with either calf intestinal phosphatase (CIP) or λPP. The *stt7* mutant[41] was used to test the involvement of the chloroplastic serine/threonine kinase STT7 in the LHCSR3 phosphorylation. In this mutant, LHCSR3 was mostly present in the non-phosphorylated form, while an STT7-independent phosphorylation was also seen in agreement with recent findings[42]. Representative dataset of an experiment replicated three times on different biological samples.

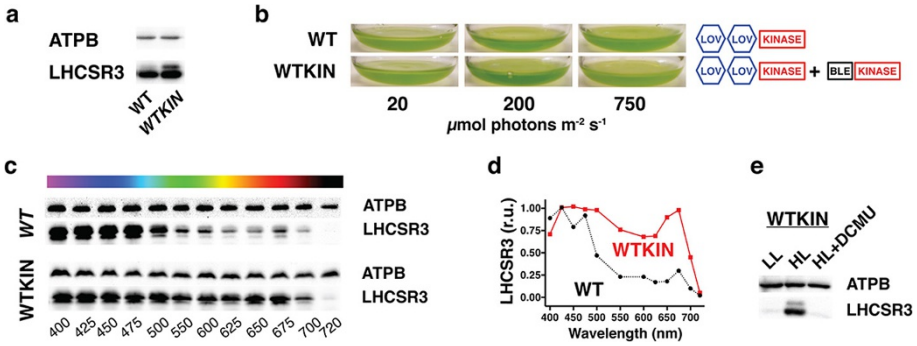

Extended Data Figure 7 | Phenotypic traits of the WTKIN genotype. **a**, Immunoblot analyses of LHCSR3 accumulation after exposure to 240 µmol photons m^{-2} s^{-1} of white light for 20 h in wild-type (137c) and WTKIN cells. ATPB was used as a loading control. **b**, Erlenmeyer flasks containing wild-type and WTKIN (expressing the kinase domain of PHOT in the wild-type background) after 20 h exposure to white light of 20, 200 and 750 µmol photons m^{-2} s^{-1} and schematic drawings of the *PHOT* gene constructs in the two lines. Representative pictures from an experiment replicated three times on different biological samples. **c**, Action spectrum of LHCSR3 accumulation in wild-type and WTKIN. ATPB was used as a loading control. **d**, Densitometric quantification of LHCSR3 accumulation in wild-type (137c) and WTKIN (data normalized to ATPB). **e**, LHCSR3 protein accumulation in WTKIN at low and high light intensity in the absence and presence of the PSII inhibitor DCMU. Representative dataset of experiment replicated three times on different biological samples.

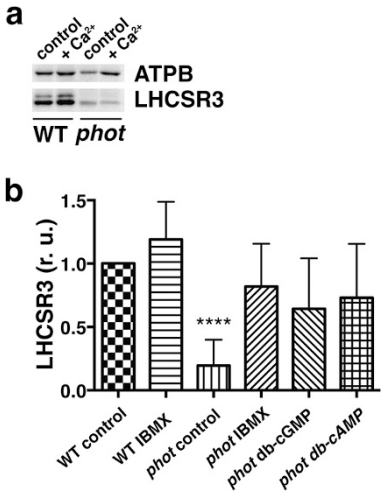

Extended Data Figure 8 | Second messengers involved in the PHOT-dependent regulation of LHCSR3 expression. a, Immunoblotting analyses of LHCSR3 accumulation after exposure to high-intensity white light for 20 h in wild-type (cw15-302) and *phot* cells under control conditions (0.34 mM Ca^{2+}) or in the presence of increased Ca^{2+} concentration (3.4 mM Ca^{2+}). Representative dataset of an experiment replicated three times on different biological samples. **b**, Statistical analyses of LHCSR3 accumulation in high-light-intensity-treated wild-type or *phot* cells in the absence (control) and presence of IBMX, DB-cGMP and DB-cAMP (see conditions as in Fig. 4a). Data are normalized to LHCSR3 levels of wild-type control cells ($n = 5$ biological samples, mean ± s.d.). Asterisks indicate statistically significant difference from wild-type control cells (*t*-test, $P < 0.0001$)

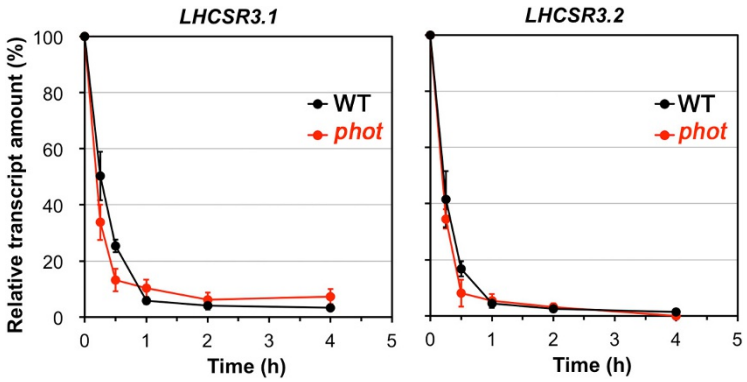

Extended Data Figure 9 | *LHCSR3.1* and *LHCSR3.2* transcript stability in wild-type and *phot* cells. Relative amounts of *LHCSR3.1* and *LHCSR3.2* mRNA in wild-type (cw15-302; black) and *phot* (red) cells were quantified by quantitative PCR. Cells exposed for 20 h to 470 nm LED light at 100 μmol photons m^{-2} s^{-1} were transfered to darkness at $t = 0$ and treated with actinomycin D to stop further mRNA synthesis. mRNA samples were collected at 0, 0.25, 0.5, 1, 2 and 4 h after transition to darkness. *LHCSR3.1* and *LHCSR3.2* transcript amounts were normalized to the amounts of 18S rRNA as endogenous control and their values were set at 100% at $t = 0$ ($n = 3$ biological samples, mean ± s.d.).

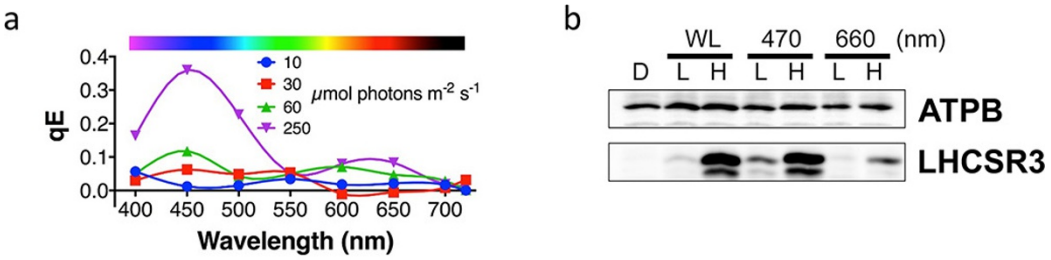

Extended Data Figure 10 | qE and LHCSR3 induction requires high light in *C. reinhardtii*. **a**, Action spectrum of qE induction in wild-type cells as a function of the light intensity. **b**, Immunoblot analysis of LHCSR3 accumulation in darkness (D) and under white (WL), blue (470 nm) and red (660 nm) light of low (20 μmol photons $m^{-2} s^{-1}$) and high intensity (250 μmol photons $m^{-2} s^{-1}$). ATPB was used as a loading control. Representative dataset of an experiment replicated two times on different biological samples.